Journal of Fluids and Structures 17 (2003) 1111–1121

JOURNAL OF FLUIDS AND STRUCTURES

www.elsevier.nl/locate/jnlabr/yjfls

Design of a tunnel-entrance hood with multiple windows and variable cross-section

M.S. Howe*

College of Engineering, Boston University, 110 Cummington Street, Boston, MA 02215, USA

Received 6 August 2002; accepted 19 April 2003

Abstract

A theory is proposed for the design of a uniform tunnel-entrance hood whose cross-sectional area $\mathscr{A}_h$ exceeds the tunnel area $\mathscr{A}$. A train entering the tunnel produces a low-frequency compression wave that can be subject to nonlinear steepening in a long tunnel. An optimized hood of length ℓ_h increases the initial thickness of the compression wave front from $\sim R/M$ to ℓ_h/M, where $R \ll \ell_h$ is the nominal radius of the tunnel and M is the train Mach number. In addition, the pressure rise should be linear across the wave front to obtain an overall minimum value of the subjectively important pressure gradient. This is achieved in a uniform hood by distributing windows along the hood wall to vent away high-pressure air displaced by the train. We consider the problem of determining the distribution and sizes of these windows and the magnitude of the area ratio $\mathscr{A}_h/\mathscr{A}$ to ensure that the hood behaves optimally at low-train Mach numbers ($M < 0.2$), when the hood can be regarded as being acoustically compact. At the projected higher Mach numbers of advanced high-speed trains (~ 0.4, say) recent analysis for hoods of uniform cross-section by Howe in 2003 indicates that a hood optimized for low Mach number operations continues to produce an essentially linear pressure rise across a compression wave of thickness $\sim \ell_h/M$ except for a low-amplitude oscillation at the very front of the wave.

1. Introduction

The amplitude of the acoustic compression wave produced when a train enters a tunnel is given approximately by

$$\Delta p \sim \frac{\rho_0 U^2}{(1-M^2)}\frac{\mathscr{A}_0}{\mathscr{A}}\left(1+\frac{\mathscr{A}_0}{\mathscr{A}}\right). \tag{1.1}$$

Δp is the pressure rise across the wave front, ρ_0 the mean air density, U the train speed, $M = U/c_0$ the train Mach number (c_0 = speed of sound in air), and the ratio $\mathscr{A}_0/\mathscr{A}$ of the train cross-sectional area $\mathscr{A}_0$ to that $\mathscr{A}$ of the tunnel is called the 'blockage' (Hara, 1961; Hara et al., 1968; Ozawa et al., 1976, 1991; Ozawa and Maeda, 1988a; Woods and Pope 1976). Δp typically exceeds 2% or 3% of the atmospheric pressure when $U > 250$ km/h (150 mile/h).

For an unmodified tunnel portal of radius R (the radius of the equivalent semi-circular tunnel of the same cross-sectional area), the pressure rise occurs over a wave front of thickness $\sim R/M$. The wave front is subject to nonlinear steepening in a long, 'smooth' tunnel with concrete slab tracks, which leads to a large increase in the amplitude of the *micro-pressure wave* radiated from the far end of the tunnel when the compression wave arrives. This wave can cause undesirable 'rattles' and vibrations in buildings near the tunnel exit.

Effective mitigation of the micro-pressure wave is achieved in practice by artificially increasing the initial thickness of the compression wave front by the addition of a 'hood' ahead of the tunnel entrance. This is a thin-walled extension

*Corresponding author. Tel.: +1-617-484-0656; fax: +1-617-353-5866.
E-mail address: mshowe@bu.edu (M.S. Howe).

0889-9746/03/$ - see front matter
doi:10.1016/S0889-9746(03)00067-7

usually fitted with 'windows' through which high-pressure air in front of the train is vented to the open-air (Ozawa et al., 1991; Maeda et al., 1993; Iida et al., 1996). The compression wave generated by a train passing through an ideal hood of length ℓ_h will have a wave-front thickness $\sim \ell_h/M$, across which the pressure rises *linearly* (producing a uniform pressure gradient) by the full amount given by Eq. (1.1).

The original hood designs were based on experiments performed by Ozawa et al. (1978) for $\ell_h \sim 3R$ and $U < 200$ km/h ($M < 0.16$). For a hood of cross-sectional area $\mathscr{A}_h > \mathscr{A}$ with no windows, it was found that the compression wave is generated in two steps: the first step is produced when the front of the train enters the hood and the second when the train passes from the hood into the tunnel (see also Sasoh et al., 1994). The maximum pressure gradient was reduced to about half its value in the absence of the hood when $\mathscr{A}_h/\mathscr{A} \sim 1.55$, and could be decreased further to about 40% of its value with no hood by opening a suitably sized window halfway along the hood and taking $\mathscr{A}_h/\mathscr{A} \sim 1.4$.

Much longer hoods fitted with multiple windows are required to obtain comparable reductions at the very much higher speeds (up to $M = 0.4$) envisaged in the future (Ozawa et al., 1991; Ozawa and Maeda, 1988b). It is perhaps unrealistic to base the design of these hoods (i.e., the determination of hood radius and window size and spacing) entirely on model scale tests.

The author has proposed an approximate theory (Howe, 2003) for calculating the compression wave produced in a long hood with multiple windows when the hood radius $R_h = R$. The theory was applicable for $M \leqslant 0.4$. At low Mach numbers, the hood length ℓ_h is acoustically compact (i.e., small compared to the compression wave thickness $\sim \ell_h/M$) so that the motion within the hood produced by the entering train can be regarded as incompressible for the purposes of calculation. A hood designed for optimal operation at small Mach numbers (i.e., one producing a compression wave with a uniformly small pressure gradient across the wave front) ceases to be optimal when M exceeds about 0.2. However, the overall changes in the waveform with increasing Mach numbers are small (Howe, 2003), so that a hood optimized for low Mach number operation constitutes a useful candidate design that can be refined by experiment.

In this paper, we extend that part of the theory of Howe (2003) concerned with *low Mach number* operations to the more practical case where $R_h > R$, and ignore the behaviour at higher Mach numbers. The design strategy then involves the use of the low Mach number theory to obtain a first approximation for the optimal window size and spacing and for the value of the ratio R_h/R. This is arguably a sensible approach, since it appears that no simple theory can conveniently incorporate the influence on the waveform of vorticity in the jet flows from the windows, whose contribution becomes progressively more important at higher train speeds. Further refinements that account for this vorticity and for higher Mach numbers can then be made by 'iterating' from the theoretically predicted optimum by systematic model scale experiments.

2. The compression wave at low Mach numbers

The analysis will be framed in terms of a model scale experimental configuration in which the tunnel consists of a circular cylindrical, rigid-walled tube of radius R and cross-sectional area $\mathscr{A} = \pi R^2$ fitted axisymmetrically with a cylindrical hood of length ℓ_h. The hood has radius $R_h > R$, and there are N windows distributed along a sidewall parallel to the hood axis (Fig. 1). Take coordinate axes $\mathbf{x} = (x, y, z)$ with the origin O in the entrance plane of the hood, with the x-axis coaxial with the cylinder and directed out of the tunnel. Let the centroid of the nth window be at $x = x_n,\ y = 0,\ z = R_h$ $(1 \leqslant n \leqslant N)$, $-\ell_h < x_N < x_{N-1} < \cdots < x_1 < 0$. The window at x_n may be regarded as curvilinear rectangular with length $\ell_x \equiv \ell_x(x_n)$ parallel to the cylinder axis and azimuthal length $\ell_\theta \equiv \ell_\theta(x_n)$.

An axisymmetric model train of maximum radius h is projected into the tunnel from $x > 0$ at uniform speed U, travelling along a tightly stretched steel wire that extends along the tunnel axis and passes through a smooth cylindrical hole along the train axis. For the purpose of calculation, the tunnel can be assumed to extend to $x = -\infty$, and the train regarded as semi-infinite, with uniform circular cross-sectional area $\mathscr{A}_0 = \pi h^2$ to the rear of the nose of length L (see figure).

In the case of an optimally designed hood, the initial pressure rise across the front of the compression wave occurs over a distance $\sim \ell_h/M$ that greatly exceeds the hood length ℓ_h when M is small. The hood is then said to be *compact*, and the distribution of pressure $p(x, t)$ within the wave front, in the tunnel ($x < -\ell_h$) ahead of the train, can be represented approximately by (Howe et al., 2000)

$$p(x,t) \approx \frac{\rho_0 U^2}{(1-M^2)\mathscr{A}}\left(1 + \frac{\mathscr{A}_0}{\mathscr{A}}\right)\int_{-\infty}^{\infty} \frac{\partial \mathscr{A}_T}{\partial x'}(x' + U[t])\frac{\partial \varphi^*}{\partial x'}(x', 0, 0)\,\mathrm{d}x', \tag{2.1}$$

provided the contributions from the low Mach number vortex sources in the exit flows from the windows are ignored. In this formula, $[t] = t + (x - \ell_h')/c_0$ is the effective retarded time, where ℓ_h' is the portal 'end correction' (Howe, 1998a;

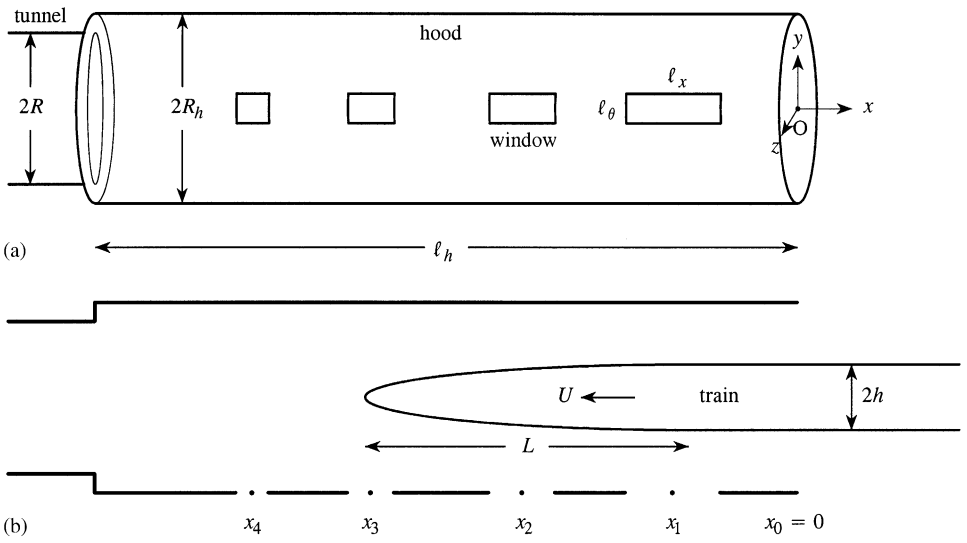

Fig. 1. (a) Circular cylindrical tunnel of radius R fitted with a hood of length ℓ_h and radius R_h with $N = 4$ rectangular windows. The geometric centre of the nth window is at $x = x_n$, $y = 0$, $z = R_h$. (b) Axisymmetric train entering the hood at speed U along the centre-line of the tunnel.

Lord Rayleigh, 1926) and $\mathscr{A}_T(s)$ is the cross-sectional area of the train at distance s from the front of the nose of the train. The latter is assumed to cross the entrance plane of the hood ($x = 0$) at time $t = 0$. The integrand vanishes except in the neighbourhood of the retarded position of the nose region of length L, where the cross-sectional area of the train varies.

The function $\varphi^*(\mathbf{x})$ originates from the formula for the *compact* acoustic Green's function that governs the production of sound by a point source in the vicinity of the hood (see Howe (1998a) for a general discussion). It is a solution of Laplace's equation that has the simple physical interpretation as the velocity potential of incompressible flow out of the tunnel portal (the irrotational flow streaming from the windows and the mouth of the hood), and is normalized such that

$$\frac{\partial \varphi^*}{\partial x} \sim 1 \quad \text{as } x \to -\infty \text{ within the tunnel,}$$
$$\varphi^* \sim -\frac{\mathscr{A}}{4\pi|\mathbf{x}|} \quad \text{as } |\mathbf{x}| \to \infty \text{ outside the portal.} \tag{2.2}$$

It is assumed that the circulation $\oint_C \nabla\varphi^* \cdot \mathrm{d}\mathbf{x} = 0$, where C is any closed contour (such as one threading two or more hood windows). The function $\varphi^*(\mathbf{x})$ accordingly is determined entirely by the geometry of the tunnel portal and hood, and the integrand in Eq. (2.1) expresses the compression wave in terms of an interaction between a moving body of variable shape (which is otherwise equivalent to distributions of monopole and dipole sources on the surface of the train) and the variable geometry of the hood.

Solution (2.1) is derived from a slender body approximation to the distribution of monopoles and dipoles that represent the train, in which these sources are replaced by a line source distributed along the train axis within the interval of length L where the train cross-section varies. Previous studies (Howe, 1998b; Howe, et al., 2000) indicate that it is valid for $\mathscr{A}_0/\mathscr{A} < 0.2$, and also for $M \leqslant 0.4$ provided the portal remains compact at the larger Mach numbers.

The compression wave is formed by the successive interactions of the train nose with the hood portal, with the windows, and finally with the junction between the hood and tunnel where there is a discontinuous change from R_h to R in the cylinder radius. It is convenient to isolate these interactions by using Eq. (2.1) to calculate $\partial p/\partial t$ instead of p. The partial derivative $\partial p/\partial t$ is conventionally referred to as the *pressure gradient*; it is small except in the vicinity of the compression wave front. Thus (after differentiation under the integral sign and integration by parts), we find

$$\frac{\partial p}{\partial t} \approx \frac{-\rho_0 U^3}{(1-M^2)\mathscr{A}}\left(1 + \frac{\mathscr{A}_0}{\mathscr{A}}\right)\int_{-\infty}^{\infty} \frac{\partial \mathscr{A}_T}{\partial x'}(x' + U[t])\frac{\partial^2 \varphi^*}{\partial x'^2}(x', 0, 0)\,\mathrm{d}x', \quad x \ll -\ell_h. \tag{2.3}$$

This formula shows that substantial changes in the pressure gradient will be observed for those retarded positions of the train nose where $\partial^2\varphi^*/\partial x'^2$ is large, namely within the hood where there are significant 'discontinuities' in hood geometry (at the portal, near windows, at the contraction in area). When $\partial p/\partial t$ has been evaluated the pressure p is computed from

$$p = \int_{-\infty}^{t} \frac{\partial p}{\partial t'}\,\mathrm{d}t'. \tag{2.4}$$

3. Approximate representation of $\varphi^*(\mathbf{x})$

The function φ^* satisfies Laplace's equation

$$\nabla^2\varphi^* = 0, \tag{3.1}$$

subject to conditions (2.2). Eq. (3.1) must normally be solved numerically because of the presence of the windows, but here we shall apply an approximate procedure in which the behaviour of $\partial^2\varphi^*/\partial x^2$ along the track of the train is determined in two stages I and II. In the first stage, the windows are replaced by a continuous sink distributed along the hood and a solution is derived for an approximation $\varphi_{\mathrm{I}}^*(x)$ within the hood which satisfies an averaged form of Eq. (3.1). This solution therefore depends only on the axial position x within the hood, and can subsequently be used to determine the 'source strength' of the individual windows. Indeed, when the size and shape of the nth window are specified the volume flux q_n through the window *directed out of the hood* is given approximately by Rayleigh's formula (Howe, 1998a; Rayleigh, 1926)

$$q_n = -K_n\varphi_{\mathrm{I}}^*(x_n), \tag{3.2}$$

where K_n is the *conductivity* of the window, and the analytic extension of $\varphi^*(\mathbf{x})$ in the free space region *outside* the hood is assumed to be negligible (so that the effective potential difference across the nth window is $-\varphi_{\mathrm{I}}^*(x_n)$). When q_n has been found for each window, a second approximation that yields $\partial^2\varphi^*/\partial x^2$ for use in Eq. (2.3) can then be obtained by introducing exact representations in the hood for the potential fields of the window sources.

3.1. Stage I

The one-dimensional, averaged equation satisfied by φ_{I}^* is

$$\frac{\partial^2\varphi_{\mathrm{I}}^*}{\partial x^2} = -Q, \tag{3.3}$$

within the hood in the interval $x_N < x < 0$ occupied by the windows (the region labelled H in Fig. 2). The continuum approximation Q to the window source strength must be taken to be constant for an optimized hood, in which case Eq. (2.3) will yield a pressure gradient that is also approximately constant and a pressure that grows linearly across the compression wave front (see also Howe, 1999). Therefore,

$$\varphi_{\mathrm{I}}^* = -\frac{Qx^2}{2} + \alpha x + \beta, \quad x_N < x < 0, \tag{3.4}$$

where α, β are constants, and this expression must match at $x \sim x_N - 0$ the velocity potential describing incompressible flow through the junction (J in Fig. 2) of the tunnel and hood. Let the latter potential be specified by

$$\varphi^* = \varphi_J^*(\mathbf{x}) + \gamma, \tag{3.5}$$

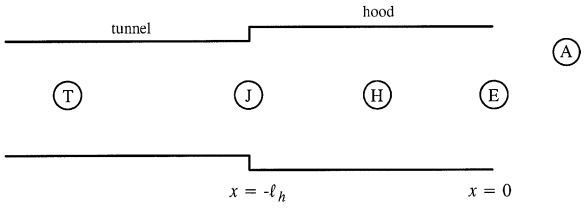

Fig. 2. The regions T, J, H, E, and A of the tunnel and hood used to define the Stage I approximation of φ^*. The coordinate origin is at the hood entrance plane.

where γ is another constant, and where the functional form of $\varphi_J^*(\mathbf{x})$ is fixed by the conditions (consistent with the behaviour defined by Eq. (2.2))

$$\varphi_J^* \sim \begin{cases} x + \ell_h - \ell_J & \text{as } x + \ell_h \to -\infty, \\ \dfrac{\mathscr{A}}{\mathscr{A}_h}(x + \ell_h) & \text{as } x + \ell_h \to \infty, \end{cases} \tag{3.6}$$

where the limiting values are attained at distances $\sim O(R_h - R)$ from the junction, and $\ell_J \ll R$ is the effective 'length' of the junction (see Howe et al., 2003). The variation of $\varphi_J^*(\mathbf{x})$ can be found in a routine manner using, for example, a finite difference approximation to the equations for potential flow through a discontinuous change in cross-section in a circular duct infinite in both directions.

Thus, equating the respective values of φ^* and $\partial\varphi^*/\partial x$ given by Eqs. (3.4) and (3.5) at $x = x_N$, we have

$$\begin{aligned} -\frac{Qx_N^2}{2} + \alpha x_N + \beta &= \frac{\mathscr{A}}{\mathscr{A}_h}(x_N + \ell_h) + \gamma, \\ -Qx_N + \alpha &= \frac{\mathscr{A}}{\mathscr{A}_h}. \end{aligned} \tag{3.7}$$

As $x \to 0$ (at E in Fig. 2, between the first window at $x = x_1$ and the entrance plane of the hood) we shall require φ_I^* to resemble the velocity potential of uniform incompressible flow from a circular cylindrical duct of radius R_h. Then (Howe, 1998a; Rayleigh, 1926)

$$\varphi_I^* = -V\ell', \quad \frac{\partial\varphi_I^*}{\partial x} = V, \qquad \text{as } x \to -0, \tag{3.8}$$

where $\ell' \approx 0.61R_h$ is the 'end correction' of an unflanged duct of radius R_h, and V is the mean flow speed $\partial\varphi_I^*/\partial x$ at the portal. These conditions yield

$$\alpha = V \quad \text{and} \quad \beta = -V\ell', \tag{3.9}$$

so that in terms of V, Eqs. (3.7) and (3.9) imply that

$$\begin{aligned} Q &= -\frac{1}{x_N}\left(\frac{\mathscr{A}}{\mathscr{A}_h} - V\right), \\ \gamma &= \frac{x_N}{2}\left(\frac{\mathscr{A}}{\mathscr{A}_h} - V\right) + V(x_N - \ell') - \frac{\mathscr{A}}{\mathscr{A}_h}(x_N + \ell_h). \end{aligned} \tag{3.10}$$

These results supply the following representations of the averaged, stage I, approximation to the velocity potential

$$\varphi^* = \begin{cases} \varphi_J^*(\mathbf{x}) + \dfrac{x_N}{2}\left(\dfrac{\mathscr{A}}{\mathscr{A}_h} - V\right) + V(x_N - \ell') - \dfrac{\mathscr{A}}{\mathscr{A}_h}(x_N + \ell_h) & \text{at T and J,} \\ \varphi_I^*(x) \equiv \dfrac{x^2}{2x_N}\left(\dfrac{\mathscr{A}}{\mathscr{A}_h} - V\right) + V(x - \ell') & \text{in the hood H,} \\ V\varphi_E^*(\mathbf{x}) & \text{at E and A,} \end{cases} \tag{3.11}$$

where T, J, H, E and A are the tunnel, hood and exterior regions shown in Fig. 2. The value of the coefficient V is arbitrary at this stage, and must be determined to optimize the behaviour of the hood (see Section 4.2). The potential function $\varphi_E^*(\mathbf{x})$ is known in analytic form for an unflanged circular duct (Eqs. (3.16) below) and may be interpreted as the velocity potential of the axisymmetric, incompressible flow from the hood portal that satisfies

$$\begin{aligned} &\frac{\partial\varphi_E^*}{\partial x} \sim 1 \quad \text{for } x \ll -R_h \text{ within the hood,} \\ &\varphi_E^* \sim -\frac{\mathscr{A}_h}{4\pi|\mathbf{x}|} \quad \text{for } |\mathbf{x}| \gg R_h \text{ outside the portal at A.} \end{aligned} \tag{3.12}$$

As $x \to -\infty$ in the tunnel, $\varphi^* \to x - \ell_h'$, where the first line of Eq. (3.11) yields the end correction in the form

$$\ell_h' \approx -\ell_h + \ell_J' + \frac{\mathscr{A}}{\mathscr{A}_h}\left(\ell_h + \frac{x_N}{2}\right) + V\left(\ell' - \frac{x_N}{2}\right). \tag{3.13}$$

3.2. Stage II

Approximation (3.11) is next refined by replacing the smoothed, collective contribution of the windows within the hood (represented by the second line of Eq. (3.11)) by terms representing the separate contributions of each window.

Let q_n denote the volume flux, defined as in Eq. (3.2), from the nth window (with centroid $x = x_n$, $1 \leqslant n \leqslant N$). It is equal to the net change in the axial volume flux within the hood between $x = x_n$ and $x = x_{n-1}$, so that

$$q_n = \mathscr{A}_h\left\{\frac{\partial\varphi_{\mathrm{I}}^*}{\partial x}(x_n) - \frac{\partial\varphi_{\mathrm{I}}^*}{\partial x}(x_{n-1})\right\} = \mathscr{A}_h\left(\frac{\mathscr{A}}{\mathscr{A}_h} - V\right)\frac{(x_n - x_{n-1})}{x_N}, \quad n = 1, 2, \ldots, N, \tag{3.14}$$

where $x_0 = 0$ (as in Fig. 1).

This result can now be used to evaluate the influence of the windows on the pressure gradient $\partial p/\partial t$ of Eq. (2.3). In the continuum approximation of stage I, Eq. (3.11) implies that $\partial^2\varphi^*/\partial x^2$ is constant within the hood, whereas it actually is approximately zero in those sections of the hood *between* neighbouring windows. To account for this behaviour, the averaged variation of φ^* within the hood (represented by $\varphi_{\mathrm{I}}^*(x)$) is replaced by the sum of the separate contributions from windows, the contribution from the nth window being set equal to the velocity potential of the incompressible flow produced by a *point sink* of strength q_n at the centroid $(x_n, 0, R_h)$ of the window in an infinite duct of radius R_h, which we write in the form

$$\frac{q_n}{\mathscr{A}_h}\varphi_n^*(\mathbf{x}).$$

In terms of cylindrical polar coordinates (r, θ, x), where $(z, y) = r(\cos\theta, \sin\theta)$, it can be shown by routine calculation (Howe, 2003; Noble, 1958) that

$$\frac{\partial^2\varphi_n^*}{\partial x^2}(r, \theta, x) = -\frac{1}{\pi R_h}\sum_{m=0}^{\infty}\int_0^{\infty}\frac{\sigma_m\lambda\cos(m\theta)}{\mathrm{I}_{m+1}(\lambda) + \mathrm{I}_{m-1}(\lambda)}\mathrm{I}_m\left(\frac{\lambda r}{R_h}\right)\cos\left(\frac{\lambda(x - x_n)}{R_h}\right)\mathrm{d}\lambda, \quad r < R_h, \tag{3.15}$$

where I_ν is a modified Bessel function (Abramowitz and Stegun, 1970), and $\sigma_0 = 1$, $\sigma_m = 2$ $(m \geqslant 1)$.

A similar integral representation is available (Howe, 1999) for the second derivative $\partial^2\varphi_E^*(\mathbf{x})/\partial x^2$ of the velocity potential representing potential flow from the hood portal, namely

$$\begin{aligned}\frac{\partial^2\varphi_E^*}{\partial x^2}(r, \theta, x) &= -\frac{1}{2\pi R_h}\int_0^{\infty}\lambda\mathrm{I}_0\left(\frac{\lambda r}{R_h}\right)\left(\frac{2\mathrm{K}_1(\lambda)}{\mathrm{I}_1(\lambda)}\right)^{1/2}\cos\left\{\lambda\left(\frac{x}{R_h} + \mathscr{Z}(\lambda)\right)\right\}\mathrm{d}\lambda, \quad r < R_h,\\ \mathscr{Z}(\lambda) &= \frac{1}{\pi}\int_0^{\infty}\ln\left(\frac{\mathrm{K}_1(\mu)\mathrm{I}_1(\mu)}{\mathrm{K}_1(\lambda)\mathrm{I}_1(\lambda)}\right)\frac{\mathrm{d}\mu}{\mu^2 - \lambda^2}\end{aligned} \tag{3.16}$$

where K_1 is a modified Bessel function (Abramowitz and Stegun, 1970). The remaining potential function $\varphi_J^*(\mathbf{x})$ in Eq. (3.11) must be found by numerical integration of Laplace's equation, as discussed above.

Taking account of these definitions, the stage II approximation yields the following representation of the second derivative $\partial^2\varphi/\partial x^2$ for use in Eq. (2.3):

$$\frac{\partial^2\varphi^*}{\partial x^2}(\mathbf{x}) = \frac{\partial^2\varphi_J^*}{\partial x^2}(\mathbf{x}) + \left(\frac{\mathscr{A}}{\mathscr{A}_h} - V\right)\sum_{n=1}^{N}\frac{(x_n - x_{n-1})}{x_N}\frac{\partial^2\varphi_n^*}{\partial x^2}(r, \theta, x) + V\frac{\partial^2\varphi_E^*}{\partial x^2}(r, \theta, x). \tag{3.17}$$

The terms on the right-hand side are, respectively, nonzero near the junction of the hood and tunnel, near the nth window $(1 \leqslant n \leqslant N)$, and at the hood portal: $\varphi_J^*(\mathbf{x})$ depends only on the area ratio $\mathscr{A}/\mathscr{A}_h$; the contributions from the windows depend on V, $\mathscr{A}/\mathscr{A}_h$ and window distribution x_n; the value of V remains to be specified.

3.3. Window dimensions

Rayleigh's formula (3.2) is used to estimate the size of the nth window. It will be assumed that the area $\mathscr{A}_n$ of the nth window is small compared to the cross-section $\mathscr{A}_h$ of the hood, and that the hood wall has thickness ℓ_w. Then according to Rayleigh (1926), the conductivity K_n satisfies

$$\frac{1}{K_n} \approx \sqrt{\frac{\pi}{4\mathscr{A}_n}} + \frac{\ell_w}{\mathscr{A}_n}. \tag{3.18}$$

Therefore,

$$\mathscr{A}_n \approx \frac{\pi K_n^2}{16}\left(1 + \sqrt{1 + \frac{16\ell_w}{\pi K_n}}\right)^2, \tag{3.19}$$

where (using the second line of Eq. (3.11) and Eq. (3.14) in Eq. (3.2))

$$K_n = \frac{\mathscr{A}_h(x_{n-1} - x_n)}{x_n^2/2 + Vx_N(x_n - \ell')/((\mathscr{A}/\mathscr{A}_h) - V)}. \tag{3.20}$$

4. Evenly spaced windows

4.1. Formulae

Suppose the hood has N evenly spaced windows with neighbouring centroids distance $\ell_h/(N+1)$ apart, such that

$$x_n = \frac{-n\ell_h}{N+1}, \quad 1 \leqslant n \leqslant N. \tag{4.1}$$

Then $\ell_h/(N+1)$ is also the distance of the innermost window at $x = x_N$ from the junction with the tunnel. Eqs. (3.14) and (3.20) imply that the corresponding window source strengths and conductivities are, respectively,

$$q_n = \frac{\mathscr{A}_h}{N}\left(\frac{\mathscr{A}}{\mathscr{A}_h} - V\right), \quad 1 \leqslant n \leqslant N, \tag{4.2}$$

and

$$K_n = \frac{2(N+1)\mathscr{A}_h}{n^2\ell_h + 2NV(n\ell_h + (N+1)\ell')/((\mathscr{A}/\mathscr{A}_h) - V)}, \quad 1 \leqslant n \leqslant N. \tag{4.3}$$

Similarly, Eq. (3.17) reduces to

$$\frac{\partial^2\varphi^*}{\partial x^2}(\mathbf{x}) = \frac{\partial^2\varphi_J^*}{\partial x^2}(\mathbf{x}) + \frac{1}{N}\left(\frac{\mathscr{A}}{\mathscr{A}_h} - V\right)\sum_{n=1}^{N}\frac{\partial^2\varphi_n^*}{\partial x^2}(r,\theta,x) + V\frac{\partial^2\varphi_E^*}{\partial x^2}(r,\theta,x). \tag{4.4}$$

4.2. Parameter values for an optimized hood

As x increases from $-\ell_h$ to 0 within an optimally designed hood $\partial\varphi^*/\partial x$ is required to decrease *linearly* from 1 to V (Howe, 1999; Howe et al., 2000). This is not possible in a hood with a discrete (as opposed to a continuum) distribution of windows. For evenly spaced windows, however, it can be closely approximated by choosing V so that the mean value of $R_h\partial^2\varphi^*/\partial x^2$ is approximately constant within the hood.

For each n and fixed values of r and θ, it follows from Eq. (3.15) that $-R_h\partial^2\varphi_n^*/\partial x^2$ is an even function of $x - x_n$, with a single positive maximum at $x = x_n$. This maximum value is approximately equal to 0.89 on the axis of symmetry. Thus, for evenly spaced windows the contribution from the series of N 'window' terms on the right of Eq. (4.4) defines a function of x that varies periodically from window to window within the hood, assuming equal *negative* maxima equal to

$$-\frac{0.89}{NR_h}\left(\frac{\mathscr{A}}{\mathscr{A}_h} - V\right)$$

on the hood axis.

The final term $V\partial^2\varphi_E^*/\partial x^2$ on the right of Eq. (4.4) is also negative and nonzero only near $x = 0$, where it attains a negative maximum value of $-0.64V/R_h$ on the axis of symmetry. Therefore, the *average* negative value of $\partial^2\varphi^*/\partial x^2$ can be expected to be approximately constant within the hood and at the hood portal provided $-0.64V/R_h = -(0.89/NR_h)(\mathscr{A}/\mathscr{A}_h - V)$, i.e., when

$$V = \frac{\mathscr{A}/\mathscr{A}_h}{1 + 0.72N}. \tag{4.5}$$

Similarly, the second derivative of the potential function $\varphi_J^*(\mathbf{x})$ (of flow through the junction from $x = -\infty$) is also negative, with a negative maximum near $x = -\ell_h$. Calculated values of this negative maximum on the x-axis of symmetry are displayed in Fig. 3 (black circles) for several values of $R_h/R = \sqrt{\mathscr{A}_h/\mathscr{A}}$. This variation is well described by the formula

$$\left(-R_h\frac{\partial^2\varphi_J^*}{\partial x^2}\right)_{\max} \approx \frac{0.6}{\sqrt{\mathscr{A}/\mathscr{A}_h}}(1 - (\mathscr{A}/\mathscr{A}_h)^{\sqrt{2\pi/3}}), \tag{4.6}$$

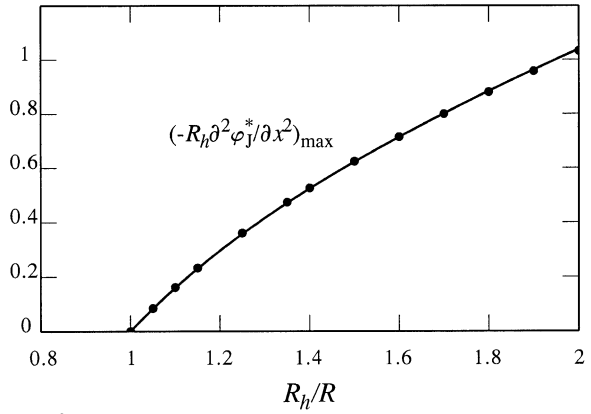

Fig. 3. Dependence of $\left(-R_h\frac{\partial^2\varphi_J^*(x,0,0)}{\partial x^2}\right)_{\max}$ on $R_h/R \equiv \sqrt{\mathscr{A}_h/\mathscr{A}}$: • • •, numerical computation;—, Eq. (4.6).

Table 1
Values of $\mathscr{A}_h/\mathscr{A}$ and R_h/R for N evenly spaced windows

N	0	1	2	3	4	5	6	7	8	9	10
$\mathscr{A}_h/\mathscr{A}$	1.636	1.389	1.281	1.220	1.181	1.154	1.134	1.118	1.106	1.096	1.088
R_h/R	1.279	1.179	1.132	1.105	1.087	1.074	1.065	1.057	1.052	1.047	1.043

which is plotted as the solid curve in Fig. 3. When the number of windows N is prescribed $(-R_h\partial^2\varphi_J^*/\partial x^2)_{\max}$ will be equal to the uniform maximum value at each of the windows and at the hood portal provided the area ratio $\mathscr{A}/\mathscr{A}_h$ is chosen to satisfy

$$\frac{0.64\mathscr{A}/\mathscr{A}_h}{1+0.72N} = \frac{0.6}{\sqrt{\mathscr{A}/\mathscr{A}_h}}(1-(\mathscr{A}/\mathscr{A}_h)^{\sqrt{2\pi/3}}). \tag{4.7}$$

The values of $\mathscr{A}_h/\mathscr{A}$ and R_h/R that satisfy this equation for $0\leqslant N\leqslant 10$ are listed in Table 1.

It is noteworthy that the values in this table of $\mathscr{A}_h/\mathscr{A}$ for $N=0$ and 1 are very close to those (1.55 and 1.4, respectively) found experimentally by Ozawa et al. (1978).

The results are illustrated further in Fig. 4 for a hood of length $\ell_h = 10R$ with $N=3$ windows, which shows the optimal behaviour of $R\partial^2\varphi^*/\partial x^2$ calculated from Eq. (4.4) on the axis of the hood (Fig. 4b) and the corresponding wavy, but essentially linear variation of $\partial\varphi^*(\mathbf{x})/\partial x$ (Fig. 4a, evaluated by integrating Eq. (4.4) from $x>0$ where $\partial\varphi^*/\partial x\to 0$). According to Table 1 and Eq. (4.5) the hood is optimal for

$$\frac{R_h}{R}\approx 1.1 \quad \text{and} \quad V\approx 0.26.$$

The five negative maxima of $R\partial^2\varphi^*/\partial x^2$ on the hood axis are seen to be of equal magnitude at roughly evenly spaced intervals. Those labelled J and E in the figure are the negative maxima produced, respectively, by the junction and hood portal potentials φ_J^* and φ_E^*; the remainder are produced by the three windows.

Eqs. (3.19) and (4.3) can be used to calculate the corresponding window dimensions. In a typical experimental arrangement the wall thickness $\ell_w\sim 0.15R$. If the windows are *square*, the nth one having side ℓ_n, we then find

$$\frac{\ell_1}{R}=0.74, \quad \frac{\ell_2}{R}=0.38, \quad \frac{\ell_3}{R}=0.25.$$

4.3. Train with ellipsoidal nose profile

The application of these results will be illustrated for the case of a train with an ellipsoidal nose profile defined by $r=h\sqrt{(x/L)(2-x/L)}$, $0<x<L$ ($r=\sqrt{y^2+z^2}$). If s denotes distance measured from the front of the train (ignoring

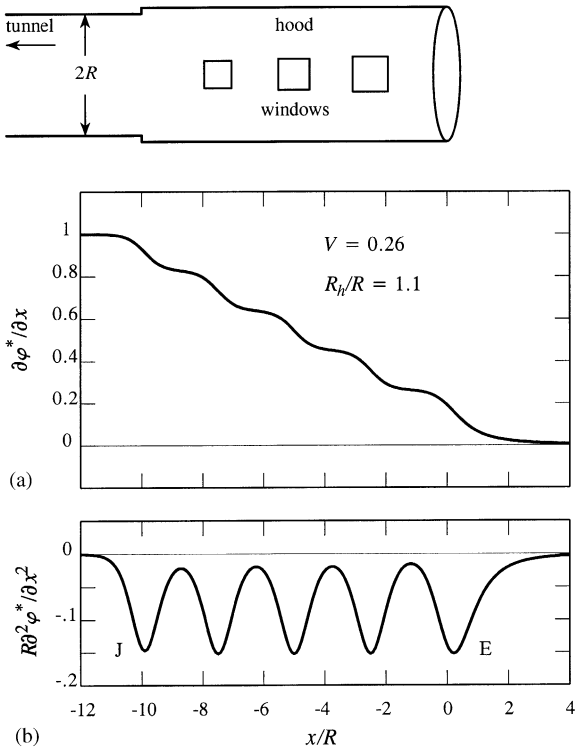

Fig. 4. Variation of (a) $\partial\varphi^*(\mathbf{x})/\partial x$ and (b) $R\partial^2\varphi^*(\mathbf{x})/\partial x^2$ on the hood axis ($r = 0$) for an optimized hood of length $\ell_h = 10R$ with $N = 3$ windows (so that $V = 0.26$ and $R_h/R \approx 1.1$).

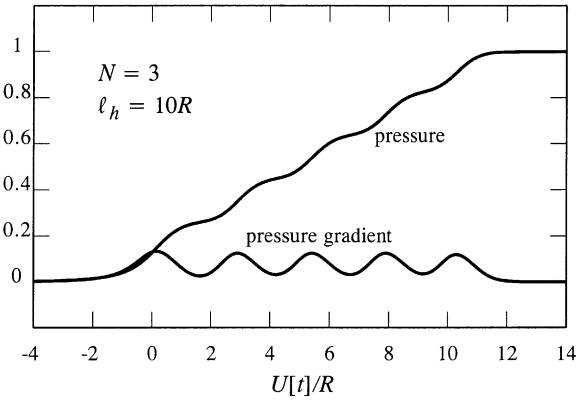

Fig. 5. The normalized compression wave pressure and pressure gradient produced by a train

$$p\Big/\frac{\rho_0 U^2}{(1-M^2)}\frac{\mathscr{A}_0}{\mathscr{A}}\Big(1+\frac{\mathscr{A}_0}{\mathscr{A}}\Big),\quad \frac{\partial p}{\partial t}\Big/\frac{\rho_0 U^3}{R(1-M^2)}\frac{\mathscr{A}_0}{\mathscr{A}}\Big(1+\frac{\mathscr{A}_0}{\mathscr{A}}\Big)$$

with the ellipsoidal nose (4.8) satisfying Eq. (4.9) entering an optimized hood of length $\ell_h = 10R$ with $N = 3$ evenly spaced windows.

the rear end of the train),

$$\frac{\mathscr{A}_T(s)}{\mathscr{A}_0} = \begin{cases} (s/L)\big(2 - s/L\big), & 0 < s < L, \\ 1, & s > L, \end{cases} \tag{4.8}$$

This formula and Eq. (4.4) have been used in Eq. (2.3) to calculate the compression wave pressure gradient $\partial p/\partial t$ for the optimized hood of length $\ell_h = 10R$, with three windows discussed above. The compression wave pressure profile is then evaluated from Eq. (2.4).

Numerical results are shown in Fig. 5 for

$$\frac{\mathscr{A}_0}{\mathscr{A}} = 0.2, \quad \frac{h}{L} = \frac{1}{3}. \tag{4.9}$$

The calculated variations of

$$p \Big/ \frac{\rho_0 U^2}{(1-M^2)} \frac{\mathscr{A}_0}{\mathscr{A}} \left(1 + \frac{\mathscr{A}_0}{\mathscr{A}}\right), \quad \frac{\partial p}{\partial t} \Big/ \frac{\rho_0 U^3}{R(1-M^2)} \frac{\mathscr{A}_0}{\mathscr{A}} \left(1 + \frac{\mathscr{A}_0}{\mathscr{A}}\right) \tag{4.10}$$

are plotted as functions of $U[t]/R$ ($[t] = t + (x - \ell'_h)/c_0$, where from Eq. (3.13) $\ell'_h \approx -3.7R$). The pressure gradient exhibits five equal maxima: that near $U[t]/R = 0$ is the contribution from $\partial^2 \varphi^*_E/\partial x^2$ produced as the nose enters the hood; that near $U[t]/R = 10$ is produced as the nose passes from the hood into the tunnel; and the three intermediate maxima are produced as the nose passes the three windows. These maxima are responsible for the 'rippling' of the pressure profile p, which otherwise rises smoothly over $-1 < U[t]/R < 11$, so that the overall compression wave thickness $\sim 12R/M$ which greatly exceeds ℓ_h when M is small.

Of course, a very much smoother pressure profile and much reduced pressure gradient maxima can be achieved by increasing the number of windows subject to conditions (4.5) and those given in Table 1.

5. Conclusion

The large-scale, low-frequency compression wave produced when a train enters a tunnel is equivalent to that generated by a combination of constant strength monopole and dipole sources translating into the tunnel at constant velocity. These sources are distributed over the nose region where the cross-sectional area of the train is variable. The compression wave is the result of the interactions of these sources with the tunnel portal. The shape of the wave-front pressure profile, and its thickness, depend critically on portal geometry, and can be modified by installation of a tunnel-entrance hood of suitable variable geometry. The overall wave-front thickness $\sim \ell_h/M$, but the wave-front profile is determined by the details of the hood geometry.

To achieve effective suppression of the micro-pressure wave pulse it is usually necessary to adjust the hood to produce an initial profile that has a *linear* rise in pressure across the wave front. For example, when $\ell_h = 10R$ this can be done by using a flared hood whose cross-sectional area decreases smoothly from $\mathscr{A}_E \approx 5.3\mathscr{A}$ at the hood entrance plane, to the tunnel area $\mathscr{A}$ at $x = -\ell_h$ according to the formula (Howe, 1999)

$$\frac{\mathscr{A}_h(x)}{\mathscr{A}} = 1 \Big/ \left[\frac{\mathscr{A}}{\mathscr{A}_E} - \frac{x}{\ell_h}\left(1 - \frac{\mathscr{A}}{\mathscr{A}_E}\right)\right], \quad -\ell_h < x < 0. \tag{5.1}$$

However, this ideal hood geometry requires the hood radius R_h at the entrance to be about $2.3R$, which is probably too large to be easily realizable at full scale.

A smoothly flared hood can be approximated by a sequence of step-like increases in cross-sectional area. The compression wave is then formed progressively by the successive interactions of the train nose with the steps. The dynamical effect of the step increases in cross-section is roughly equivalent to that produced in a hood of *constant* cross-section when the steps are replaced by suitably sized windows. This means that a combination of hood area changes and windows can be used to simulate the ideally flared geometry of Eq. (5.1). The results given in Section 4 of this paper show how this can be done for moderate train Mach numbers in the important case where the hood area $\mathscr{A}_h > \mathscr{A}$ is constant. In the special case of $N = 1$ window, or when there are no windows, our predictions of the respective optimum values of $\mathscr{A}_h/\mathscr{A}$ agree with those determined experimentally by Ozawa et al. (1978). For hoods with multiple windows, the dimensions predicted by our analysis of some of the 'inner' windows may be too small in practice, because of our implicit neglect of 'vortex' compression wave sources within the jet flows from the windows of air displaced by the moving train (cf. Howe et al., 2000). Preliminary calculations performed by the author for a *long* hood with a single window indicate that the neglect of vorticity production in the window produces a temporary drop in pressure just to the rear of the compression wave front, contrary to observation; the pressure subsequently rises to a value consistent with experiment. According to the present theory, however, such pressure drops do not occur for an optimized hood with multiple windows. Thus, it is likely that the principal defect of the irrotational approximation of this paper is that the neglect of vorticity production (which might effectively impede flow from the inner, smaller windows) will lead to a prediction of the compression wave front that is marginally thicker than that realized in practice. It will therefore be

necessary to fine-tune these predictions by using data from model-scale experiments to adjust the dimensions of the smaller windows.

At higher Mach numbers (> 0.2, say) the assumption of hood 'compactness' becomes questionable, and phase differences between the interactions of the train nose with windows at opposite ends of the hood become progressively more important. However, a detailed analysis of the effect of noncompactness for a hood of constant cross-sectional area (Howe, 2003) indicates that when M is as large as 0.4, a hood that has been optimized for low Mach number operations continues to produce an essentially linear pressure rise across compression wave of thickness $\sim \ell_h/M$ except for a low-amplitude oscillation at the very front of the wave.

Acknowledgements

The work reported in this paper is sponsored by the Japan Railway Technical Research Institute administered by Dr Eng. Tatsuo Maeda. The author gratefully acknowledges the benefit of discussions with Dr Maeda and with Dr Masanobu Iida.

References

Abramowitz, M., Stegun, I.A., (Eds.) 1970. Handbook of Mathematical Functions. National Bureau of Standards Applied Mathematics Series No. 55, US Department of Commerce (Ninth corrected printing), Washington, D.C.

Hara, T., 1961. Aerodynamic force acting on a high speed train at tunnel entrance. Quarterly Report of the Railway Technical Research Institute 2 (2), 5–11.

Hara, T., Kawaguti, M., Fukuchi, G., Yamamoto, A., 1968. Aerodynamics of high-speed train. Monthly Bulletin of the International Railway Congress Association XLV (2), 121–146.

Howe, M.S., 1998a. Acoustics of Fluid–Structure Interactions. Cambridge University Press, Cambridge.

Howe, M.S., 1998b. Mach number dependence of the compression wave generated by a high-speed train entering a tunnel. Journal of Sound and Vibration 212, 23–36.

Howe, M.S., 1999. On the compression wave generated when a high-speed train enters a tunnel with a flared portal. Journal of Fluids and Structures 13, 481–498.

Howe, M.S., 2003. Influence of train Mach number on the compression wave generated in a tunnel-entrance hood. Journal of Engineering Mathematics 46, 147–163.

Howe, M.S., Iida, M., Fukuda, T., Maeda, T., 2000. Theoretical and experimental investigation of the compression wave generated by a train entering a tunnel with a flared portal. Journal of Fluid Mechanics 425, 111–132.

Howe, M.S., Iida, M., Fukuda, T., 2003. Influence of an unvented tunnel entrance hood on the compression wave generated by a high-speed train. Journal of Fluids and Structures 17, 833–853.

Iida, M., Matsumura, T., Nakatani, K., Fukuda, T., Maeda, T., 1996. Optimum nose shape for reducing tunnel sonic boom. Institution of Mechanical Engineers Paper C514/015/96.

Maeda, T., Matsumura, T., Iida, M., Nakatani, K., Uchida, K., 1993. Effect of shape of train nose on compression wave generated by train entering tunnel. Proceedings of the International Conference on Speedup Technology for Railway and Maglev Vehicles, Yokohama, Japan, 22–26 November, 1993, pp. 315–319.

Noble, B., 1958. Methods based on the Wiener–Hopf Technique. Pergamon, London (Reprinted 1988 by Chelsea Publishing Company, New York).

Ozawa, S., Maeda, T., 1988a. Model experiment on reduction of micro-pressure wave radiated from tunnel exit. Proceedings of the International Symposium on Scale Modeling, Japan Society of Mechanical Engineers, Tokyo, 18–22 July.

Ozawa, S., Maeda, T., 1988b. Tunnel entrance hoods for reduction of micro-pressure wave. Quarterly Report of the Railway Technical Research Institute 29 (3), 134–139.

Ozawa, S., Morito, Y., Maeda, T., Kinosita, M., 1976. Investigation of the pressure wave radiated from a tunnel exit. Railway Technical Research Institute Report 1023 (in Japanese).

Ozawa, S., Uchida, T., Maeda, T., 1978. Reduction of micro-pressure wave radiated from tunnel exit by hood at tunnel entrance. Quarterly Report of the Railway Technical Research Institute 19 (2), 77–83.

Ozawa, S., Maeda, T., Matsumura, T., Uchida, K., Kajiyama, H., Tanemoto, K., 1991. Countermeasures to reduce micro-pressure waves radiating from exits of Shinkansen tunnels. In: Haerter, A. (Ed.), Aerodynamics and Ventilation of Vehicle Tunnels. Elsevier Science Publishers, Amsterdam, pp. 253–266.

Lord Rayleigh, 1926. The Theory of Sound, Vol. 2. Macmillan, London.

Sasoh, A., Onodera, O., Takayama, K., Kaneko, R., Matsui, Y., 1994. Experimental investigation on the reduction of railway sonic boom. Transactions of the Japan Society of Mechanical Engineers B60, 4112–4118 (in Japanese).

Woods, W.A., Pope, C.W., 1976. Secondary aerodynamic effects in rail tunnels during vehicle entry. Paper C5, Second BHRA Symposium of the Aerodynamics and Ventilation of Vehicle Tunnels, Cambridge, England, 23–25 March 1976, pp. 71–86.